Hindawi Publishing Corporation
Journal of Fluids
Volume 2015, Article ID 561263, 9 pages
http://dx.doi.org/10.1155/2015/561263

Research Article

Analysis of Heat and Mass Transfer on MHD Peristaltic Flow through a Tapered Asymmetric Channel

M. Kothandapani,[1] J. Prakash,[2] and V. Pushparaj[3]

[1]*Department of Mathematics, University College of Engineering Arni (A Constituent College of Anna University, Chennai), Arni, Tamil Nadu 632 326, India*
[2]*Department of Mathematics, Arulmigu Meenakshi Amman College of Engineering, Vadamavandal, Tamil Nadu 604 410, India*
[3]*Department of Mathematics, C. Abdul Hakeem College of Engineering & Technology, Melvisharam, Tamil Nadu 632 509, India*

Correspondence should be addressed to M. Kothandapani; mkothandapani@gmail.com

Received 31 August 2014; Accepted 15 December 2014

Academic Editor: Miguel Onorato

This paper describes the peristaltic flow of an incompressible viscous fluid in a tapered asymmetric channel with heat and mass transfer. The fluid is electrically conducting fluid in the presence of a uniform magnetic field. The propagation of waves on the nonuniform channel walls to have different amplitudes and phase but with the same speed is generated the tapered asymmetric channel. The assumptions of low Reynolds number and long wavelength approximations have been used to simplify the complicated problem into a relatively simple problem. Analytical expressions for velocity, temperature, and concentration have been obtained. Graphically results of the flow characteristics are also sketched for various embedded parameters of interest entering the problem and interpreted.

1. Introduction

The study of peristaltic transport has enjoyed increased interest from investigators in several engineering disciplines. From a mechanical point of view, peristalsis offers the opportunity of constructing pumps in which the transported medium does not come in direct contact with any moving parts such as valves, plungers, and rotors. This could be of great benefit in cases where the medium is either highly abrasive or decomposable under stress. This has led to the development of fingers and roller pumps which work according to the principle of peristalsis. Applications include dialysis machines, open-heart bypass pump machines, and infusion pumps. After the first investigation reported by Latham [1], several theoretical and experimental investigations [2–5] about the peristaltic flow of Newtonian and non-Newtonian fluids have been made under different conditions with reference to physiological and mechanical situations.

In view of the processes like hemodialysis and oxygenation, some progress is shown in the theory of peristalsis with heat transfer [6–8]. Such analysis of heat transfer is of great value in biological tissues, dilution technique in examining blood flow, destruction of undesirable cancer tissues, metabolic heat generation, and so forth. In addition, the mass transfer effect on the peristaltic flow of viscous fluid has been examined in the studies [9–11]. The effect of magnetic field on a Newtonian fluid has been reported for treatment of gastronomic pathologies, constipation, and hypertension.

Recently, few attempts have been made in the peristaltic literature to study the combined effects of heat and mass transfer. Eldabe et al. [10] analyzed the mixed convective heat and mass transfer in a non-Newtonian fluid at a peristaltic surface with temperature-dependent viscosity. The influence of heat and mass transfer on MHD peristaltic flow through a porous space with compliant walls was studied by Srinivas and Kothandapani [11]. The effects of elasticity of the flexible walls on the peristaltic transport of viscous fluid with heat transfer in a two-dimensional uniform channel have been investigated by Srinivas and Kothandapani [12]. Ogulu [13]

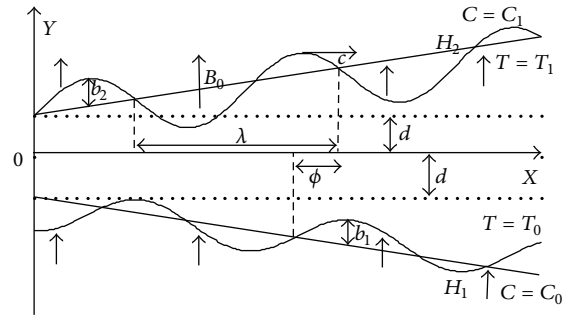

Figure 1: Schematic diagram of the tapered asymmetric channel.

examined heat and mass transfer of blood under the influence of a uniform magnetic field.

The problem of intrauterine fluid motion in a nonpregnant uterus caused by myometrial contractions is a peristaltic-type fluid motion and the myometrial contractions may occur in both symmetric and asymmetric directions. Further it is observed that the intrauterine fluid flow in a sagittal cross section of the uterus discloses a narrow channel enclosed by two fairly parallel walls with wave trains having different amplitudes and phase difference [14–16]. Keeping in view of the abovementioned reasons, a new theoretical investigation of peristaltic motion of a Newtonian fluid in the presence of heat and mass transfer in the most generalized form of the channel, namely, the tapered asymmetric channel, is carried out. The governing equations of motion, energy, and concentration are simplified by using the assumptions of long wavelength and low Reynolds number approximations. The exact solutions of velocity, temperature, and concentration of the fluid are generated. Also interesting flow quantities are analyzed by plotting various graphs.

2. Mathematical Formulation

Consider the unsteady, combined convective heat and mass transfer, MHD flow of an electrically conducting viscous fluid in a two-dimensional tapered asymmetric channel. Let $\overline{Y} = \overline{H}_1$ and $\overline{Y} = \overline{H}_2$, respectively, the lower and upper wall boundaries of the tapered asymmetric channel. The flow is generated by sinusoidal wave trains propagating with constant speed c along the tapered asymmetric channel (Figure 1). The geometry of the wall surface [15, 16] is defined as

$$\overline{H_2}\left(\overline{X},\overline{t}\right) = d + m'\overline{X} + b_2 \sin\left[\frac{2\pi}{\lambda}\left(\overline{X} - c\overline{t}\right)\right]. \quad \text{upper wall,} \tag{1a}$$

$$\overline{H_1}\left(\overline{X},\overline{t}\right) = -d - m'\overline{X} - b_1 \sin\left[\frac{2\pi}{\lambda}\left(\overline{X} - c\overline{t}\right) + \phi\right]. \quad \text{lower wall,} \tag{1b}$$

where d is the half width of the channel at the inlet, b_1 and b_2 are the amplitudes of lower and upper walls, respectively, c is the phase speed of the wave, m' ($m' \ll 1$) is the nonuniform parameter, λ is the wavelength, the phase difference ϕ varies in the range $0 \le \phi \le \pi$, $\phi = 0$ corresponds to symmetric channel with waves out of phase (i.e., both walls move towards outward or inward simultaneously), and further b_1, b_2, and ϕ satisfy the following conditions for the divergent channel at the inlet:

$$b_1^2 + b_2^2 + 2b_1 b_2 \cos(\phi) \le (2d)^2. \tag{2}$$

It is assumed that the temperature and concentration at lower wall are T_0 and C_0, respectively, while the temperature and concentration at the upper wall are T_1 and C_1, respectively ($T_0 < T_1$ & $C_0 < C_1$). The equations of continuity, momentum, energy, and concentration are described as follows [11, 12]:

$$\begin{aligned}
&\frac{\partial \overline{U}}{\partial \overline{X}} + \frac{\partial \overline{V}}{\partial \overline{Y}} = 0,\\
&\rho\left[\frac{\partial \overline{U}}{\partial \overline{t}} + \overline{U}\frac{\partial \overline{U}}{\partial \overline{X}} + \overline{V}\frac{\partial \overline{U}}{\partial \overline{Y}}\right]\\
&\quad = -\frac{\partial \overline{P}}{\partial \overline{X}} + \mu\left[\frac{\partial^2 \overline{U}}{\partial \overline{X}^2} + \frac{\partial^2 \overline{U}}{\partial \overline{Y}^2}\right] - \sigma B_0^2 \overline{U},\\
&\rho\left[\frac{\partial \overline{V}}{\partial \overline{t}} + \overline{U}\frac{\partial \overline{V}}{\partial \overline{X}} + \overline{V}\frac{\partial \overline{V}}{\partial \overline{Y}}\right] = -\frac{\partial \overline{P}}{\partial \overline{Y}} + \mu\left[\frac{\partial^2 \overline{V}}{\partial \overline{X}^2} + \frac{\partial^2 \overline{V}}{\partial \overline{Y}^2}\right],\\
&\rho\zeta\left[\frac{\partial \overline{T}}{\partial \overline{t}} + \overline{U}\frac{\partial \overline{T}}{\partial \overline{X}} + \overline{V}\frac{\partial \overline{T}}{\partial \overline{Y}}\right]\\
&\quad = \kappa\left[\frac{\partial^2 \overline{T}}{\partial \overline{X}^2} + \frac{\partial^2 \overline{T}}{\partial \overline{Y}^2}\right]\\
&\qquad + \mu\left\{2\left[\left(\frac{\partial \overline{U}}{\partial \overline{X}}\right)^2 + \left(\frac{\partial \overline{V}}{\partial \overline{Y}}\right)^2\right] + \left(\frac{\partial \overline{U}}{\partial \overline{Y}} + \frac{\partial \overline{V}}{\partial \overline{X}}\right)^2\right\},\\
&\left[\frac{\partial \overline{C}}{\partial \overline{t}} + \overline{U}\frac{\partial \overline{C}}{\partial \overline{X}} + \overline{V}\frac{\partial \overline{C}}{\partial \overline{Y}}\right]\\
&\quad = D_m\left[\frac{\partial^2 \overline{C}}{\partial \overline{X}^2} + \frac{\partial^2 \overline{C}}{\partial \overline{Y}^2}\right] + \frac{D_m K_T}{T_m}\left[\frac{\partial^2 \overline{T}}{\partial \overline{X}^2} + \frac{\partial^2 \overline{T}}{\partial \overline{Y}^2}\right],
\end{aligned} \tag{3}$$

where $\overline{U}$, $\overline{V}$ are the components of velocity along $\overline{X}$ and $\overline{Y}$ directions, respectively, $\overline{t}$ is the dimensional time, μ is the coefficient of viscosity, σ is the electrical conductivity of the fluid, B_0 is the uniform applied magnetic field, ρ is the fluid density, ζ is the specific heat at constant volume, $\overline{P}$ is the pressure, $\overline{T}$ is the temperature, $\overline{C}$ is the concentration of the fluid, T_m is the mean temperature, κ is the thermal conductivity, D_m is the coefficient of mass diffusivity, and K_T is the thermal diffusion ratio.

The corresponding boundary conditions are

$$\overline{U} = 0, \quad \overline{T} = T_0, \quad \overline{C} = C_0 \quad \text{at } \overline{Y} = \overline{H}_1, \tag{4a}$$

$$\overline{U} = 0, \quad \overline{T} = T_1, \quad \overline{C} = \overline{C}_1, \quad \text{at } \overline{Y} = \overline{H}_2. \tag{4b}$$

By introducing the following set of nondimensional variables in (3),

$$\begin{aligned} x' &= \frac{\overline{X}}{\lambda}, \quad y' = \frac{\overline{Y}}{d}, \quad t' = \frac{c\bar{t}}{\lambda}, \\ u' &= \frac{\overline{U}}{c}, \quad v' = \frac{\overline{V}}{c}, \quad \delta = \frac{d}{\lambda}, \\ h_1 &= \frac{\overline{H_1}}{d}, \quad h_2 = \frac{\overline{H_2}}{d}, \quad p' = \frac{d^2\overline{P}}{c\lambda\mu}, \\ \theta &= \frac{\overline{T} - T_0}{T_1 - T_0}, \quad \Theta = \frac{\overline{C} - C_0}{C_1 - C_0}, \end{aligned} \tag{5}$$

we obtain

$$\begin{aligned} &R\delta\left[\frac{\partial u'}{\partial t'} + u'\frac{\partial u'}{\partial x'} + v'\frac{\partial u'}{\partial y'}\right] \\ &\quad = -\frac{\partial p'}{\partial x'} + \delta^2\frac{\partial^2 u'}{\partial x'^2} + \frac{\partial^2 u'}{\partial y'^2} - M^2 u', \\ &R\delta^3\left[\frac{\partial v'}{\partial t'} + u'\frac{\partial v'}{\partial x'} + v'\frac{\partial v'}{\partial y'}\right] \\ &\quad = -\frac{\partial p'}{\partial y'} + \delta^2\left[\frac{\partial^2 v'}{\partial x'^2} + \frac{\partial^2 v'}{\partial y'^2}\right], \\ &R\delta\left[\frac{\partial \theta}{\partial t'} + u'\frac{\partial \theta}{\partial x'} + v'\frac{\partial \theta}{\partial y'}\right] \\ &\quad = \frac{1}{\mathrm{Pr}}\left[\delta^2\frac{\partial^2\theta}{\partial x'^2} + \frac{\partial^2\theta}{\partial y'^2}\right] \\ &\qquad + E\left[2\left[\delta^2\left(\left(\frac{\partial u'}{\partial x'}\right)^2 + \left(\frac{\partial v'}{\partial y'}\right)^2\right)\right]\right. \\ &\qquad \left. + \left[\frac{\partial u'}{\partial y'} + \delta\frac{\partial v'}{\partial x'}\right]^2\right], \\ &R\delta\left[\frac{\partial \Theta}{\partial t'} + u'\frac{\partial \Theta}{\partial x'} + v'\frac{\partial \Theta}{\partial y'}\right] \\ &\quad = \frac{1}{\mathrm{Sc}}\left[\delta^2\frac{\partial^2\Theta}{\partial x'^2} + \frac{\partial^2\Theta}{\partial y'^2}\right] + \mathrm{Sr}\left[\delta^2\frac{\partial^2\theta}{\partial x'^2} + \frac{\partial^2\theta}{\partial y'^2}\right], \end{aligned} \tag{6}$$

where a $(= b_1/d)$ and b $(= b_2/d)$ are nondimensional amplitudes of lower and upper walls, respectively, $k_1 = (\lambda m'/d)$ is nonuniform parameter, R $(= cd\rho/\mu)$ is the Reynolds number, $\mathrm{Sc} = \mu/D_m\rho$ is the Schmidt number, $\mathrm{Sr} = \rho D_m K_T(T_1 - T_0)/\mu(C_1 - C_0)T_m$ is the Soret number, $M = \sqrt{\sigma/\mu}B_0 d$ is the Hartmann number, $\mathrm{Pr} = \rho\nu\zeta/\kappa$ is the Prandtl number, and $E = c^2/\zeta(T_1 - T_0)$ is the Eckert number.

In order to discuss the results quantitatively, we assume the instantaneous volume rate of the flow $F(x,t)$, periodic in $(x - t)$ [17–19], as

$$F(x,t) = Q + a\sin\left[2\pi(x-t) + \phi\right] + b\sin 2\pi(x-t), \tag{7}$$

where Q is the time-average of the flow over one period of the wave and

$$F = \int_{h_1}^{h_2} u\,dy. \tag{8}$$

3. Exact Analytical Solution

Using the long wavelength approximation and neglecting the wave number along with low Reynolds number and omitting prime, one can find from (6) that

$$0 = -\frac{\partial p}{\partial x} + \frac{\partial^2 u}{\partial y^2} - M^2 u, \tag{9}$$

$$0 = -\frac{\partial p}{\partial y}, \tag{10}$$

$$0 = \frac{1}{\mathrm{Pr}}\frac{\partial^2\theta}{\partial y^2} + E\left(\frac{\partial u}{\partial y}\right)^2, \tag{11}$$

$$0 = \frac{\partial^2\Theta}{\partial y^2} + \mathrm{ScSr}\frac{\partial^2\theta}{\partial y^2}. \tag{12}$$

Equation (10) shows that p is not function of y.

The corresponding boundary conditions are

$$\begin{aligned} &u = 0, \quad \theta = 1, \text{ and } \Theta = 1 \\ &\text{at } y = h_2 = 1 + k_1 x + b\sin(2\pi(x-t)), \end{aligned} \tag{13a}$$

$$\begin{aligned} &u = 0, \quad \theta = 0, \text{ and } \Theta = 0 \\ &\text{at } y = h_1 = -1 - k_1 x - a\sin(2\pi(x-t) + \phi) \end{aligned} \tag{13b}$$

which satisfy, at the inlet of channel,

$$a^2 + b^2 + 2ab\cos(\phi) \le 4. \tag{14}$$

The set of (9)–(12), subject to the conditions (13a) and (13b), are solved exactly for u, θ, and Θ, and we have

$$\begin{aligned} u = {} & \frac{(\partial p/\partial x)}{M^2} \\ & \times\left(1 - \frac{(\cosh(Mh_2) - \cosh(Mh_1))\sinh(Mh_1)}{M^2\sinh(M(h_1 - h_2))}\right) \\ & \times\frac{\cosh(My)}{\cosh(Mh_1)} + \frac{(\partial p/\partial x)}{M^2} \\ & \times\left(\frac{(\cosh(Mh_2) - \cosh(Mh_1))\sinh(My)}{M^2\sinh(M(h_1 - h_2))} - 1\right), \end{aligned}$$

$$\theta = A_1 + B_1 y - \frac{\Pr EA^2}{8}\left[\cosh(2My) - 2y^2M^2\right] - \frac{\Pr EB^2}{8}\left[\cosh(2My) + 2y^2M^2\right] - \frac{\Pr EAB}{8}\sinh(2My),$$

$$\Theta = 4D_3\mathrm{ScSr}M^2h_1^2 - D_4h_1 - D_1\mathrm{ScSr}e^{2Mh_1} - D_2\mathrm{ScSr}e^{-2Mh_1} + D_4y + D_1\mathrm{ScSr}e^{2My} + D_2\mathrm{ScSr}e^{-2My} - 4D_3\mathrm{ScSr}M^2y^2,$$

$$\frac{\partial p}{\partial x} = FM^3\cosh(Mh_1)\sinh(M(h_1-h_2)) \times \left((\sinh(Mh_2) - \sinh(Mh_1)) \times \left[\sinh(M(h_1-h_2)) - \left[\cosh(Mh_2) - \cosh(Mh_1)\right]\sinh(Mh_1)\right]\right)^{-1} + \frac{FM^3\sinh(M(h_1-h_2))}{\left[\cosh(Mh_2) - \cosh(Mh_1)\right]^2} - \frac{FM^2}{h_2-h_1}, \tag{15}$$

where

$$A = \frac{\left((\partial p/\partial x) - BM^2\sinh(Mh_1)\right)}{M^2\cosh(Mh_1)},$$

$$B = \frac{(\partial p/\partial x)\left(\cosh(Mh_2) - \cosh(Mh_1)\right)}{M^2\sinh(M(h_1-h_2))},$$

$$A_1 = \frac{\Pr EA^2}{8}\left[\cosh(2Mh_1) - 2h_1^2M^2\right] + \frac{\Pr EB^2}{8}\left[\cosh(2Mh_1) + 2h_1^2M^2\right] + \frac{\Pr EAB}{8}\sinh\left[2Mh_1\right] - Dh_1,$$

$$B_1 = \frac{1}{h_2-h_1}\left[1 + \frac{\Pr EA^2}{8}\left[\cosh(2Mh_2) - 2h_2^2M^2 - \cosh(2Mh_1) + 2h_1^2M^2\right] + \frac{\Pr EB^2}{8}\left[\cosh(2Mh_2) + 2h_2^2M^2 - \cosh(2Mh_1) - 2h_1^2M^2\right] + \frac{\Pr EAB}{8}\left[\sinh(2Mh_2) - \sinh(2Mh_1)\right]\right],$$

$$D_1 = \frac{\Pr EA^2}{16} + \frac{\Pr EB^2}{16} + \frac{\Pr EAB}{8},$$

$$D_2 = \frac{\Pr EA^2}{16} + \frac{\Pr EB^2}{16} - \frac{\Pr EAB}{8},$$

$$D_3 = \frac{\Pr EA^2}{16} - \frac{\Pr EB^2}{16},$$

$$D_4 = \frac{1}{h_1-h_2}\left(4D_3\mathrm{ScSr}M^2\left(h_1^2 - h_2^2\right) - D_1\mathrm{ScSr}\left(e^{2Mh_1} - e^{2Mh_2}\right) - D_2\mathrm{ScSr}\left(e^{-2Mh_1} - e^{-2Mh_2}\right) - 1\right). \tag{16}$$

The coefficient of heat transfer at the lower wall is given by

$$Z = h_{1x}\theta_y. \tag{17}$$

4. Numerical Results and Discussion

The effect of various flow parameters on temperature is plotted in Figure 2 for the fixed values of $x = 0.6$ and $t = 0.4$. The influence of the nonuniform parameter (k_1) on θ is depicted in Figure 2(a). It is noticed that the temperature (θ) increases nearer to the lower wall of the tapered channel while the situation is reversed as nonuniform parameter (k_1) increases. Figure 2(b) reveals that the temperature profile increases with increase of Eckert number. It is considered from Figure 2(c) that the temperature profile increases as the amplitude of lower tapered channel increases. The variation of the Prandtl number (Pr) on θ is shown in Figure 2(d). This figure indicates that an increase in Prandtl number results in increase in the temperature of the fluid. Figure 2(e) depicts the effect of temperature for the various values of Q. It is observed that the temperature θ increases with an increase in the time-average flow rate Q in the entire tapered channel. The variations of the Hartmann number M against θ are shown in Figure 2(f). This figure indicates that by increasing the Hartmann number the temperature decreases. The result presented in Figure 3 indicates the behavior of E, a, Q, M, ϕ, and Pr on the heat transfer coefficient (Z). These figures display the typical oscillatory behavior of heat transfer which may be due to the phenomenon of peristalsis. Figures 3(a)–3(f) reveal that the absolute value of the heat transfer coefficient increases by increasing E, a, Q, M, ϕ, and Pr.

The effect of various physical parameters on the concentration of the fluid (Θ) is shown in Figure 4. Figure 4(a) exposes that the fluid concentration decreases with an increase of E. It is noticed from Figure 4(b) that the concentration of the fluid increases as a increases. Figure 4(c) shows that the absolute value of concentration distribution increases at the central part of channel when k_1 is increased. Figure 4(d) is plotted to see the influence of M on the concentration. We notice that an increase in M increases Θ. The concentration for the phase difference is shown in Figure 4(e). It is observed that an increase in ϕ causes increase in Θ. In Figure 4(f), the cause of Prandtl number Pr on Θ is captured. It is

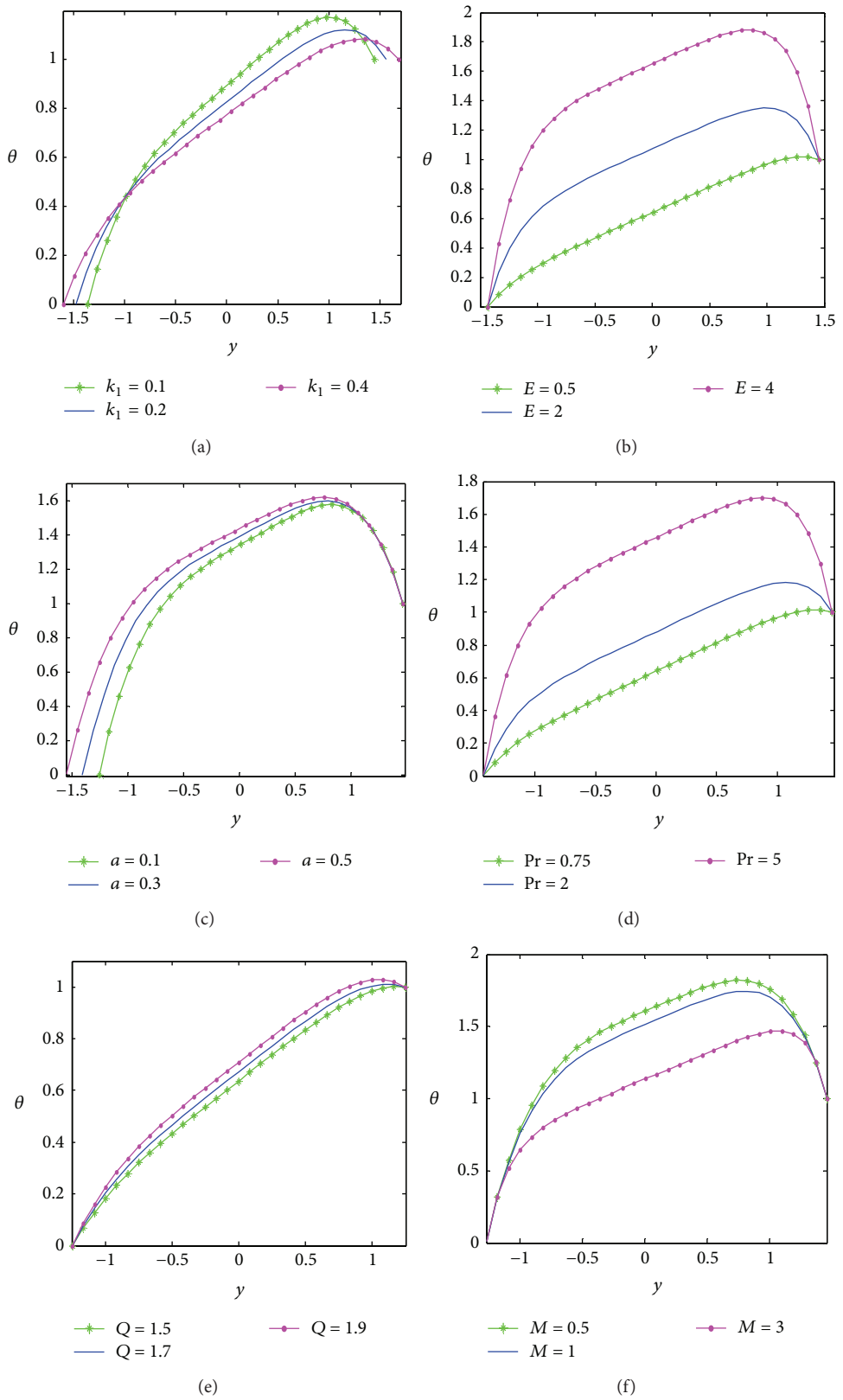

FIGURE 2: Temperature distribution (for fixed value of $t = 0.4$ and $x = 0.6$): (a) $Q = 1.7$, $\phi = \pi/3$, $M = 1$, $E = 0.5$, $\Pr = 1.7$, $a = 0.3$, and $b = 0.4$; (b) $E = 0.5$, $k_1 = 0.2$, $Q = 1.85$, $M = 2$, $\phi = \pi/4$, $a = 0.35$, and $b = 0.3$; (c) $E = 1$, $\phi = \pi/3$, $\Pr = 2$, $M = 0.5$, $k_1 = 0.3$, $Q = 1.75$, and $b = 0.3$; (d) $E = 0.5$, $k_1 = 0.2$, $Q = 1.85$, $M = 2$, $\phi = \pi/4$, $a = 0.35$, and $b = 0.3$; (e) $E = 0.7$, $\phi = \pi/6$, $\Pr = 0.6$, $k_1 = 0.25$, $M = 0.8$, $a = 0.1$, and $b = 0.2$; (f) $\phi = \pi/2$, $E = 2$, $\Pr = 1.5$, $b = 0.3$, $a = 0.2$, $k_1 = 0.3$, and $Q = 1.6$.

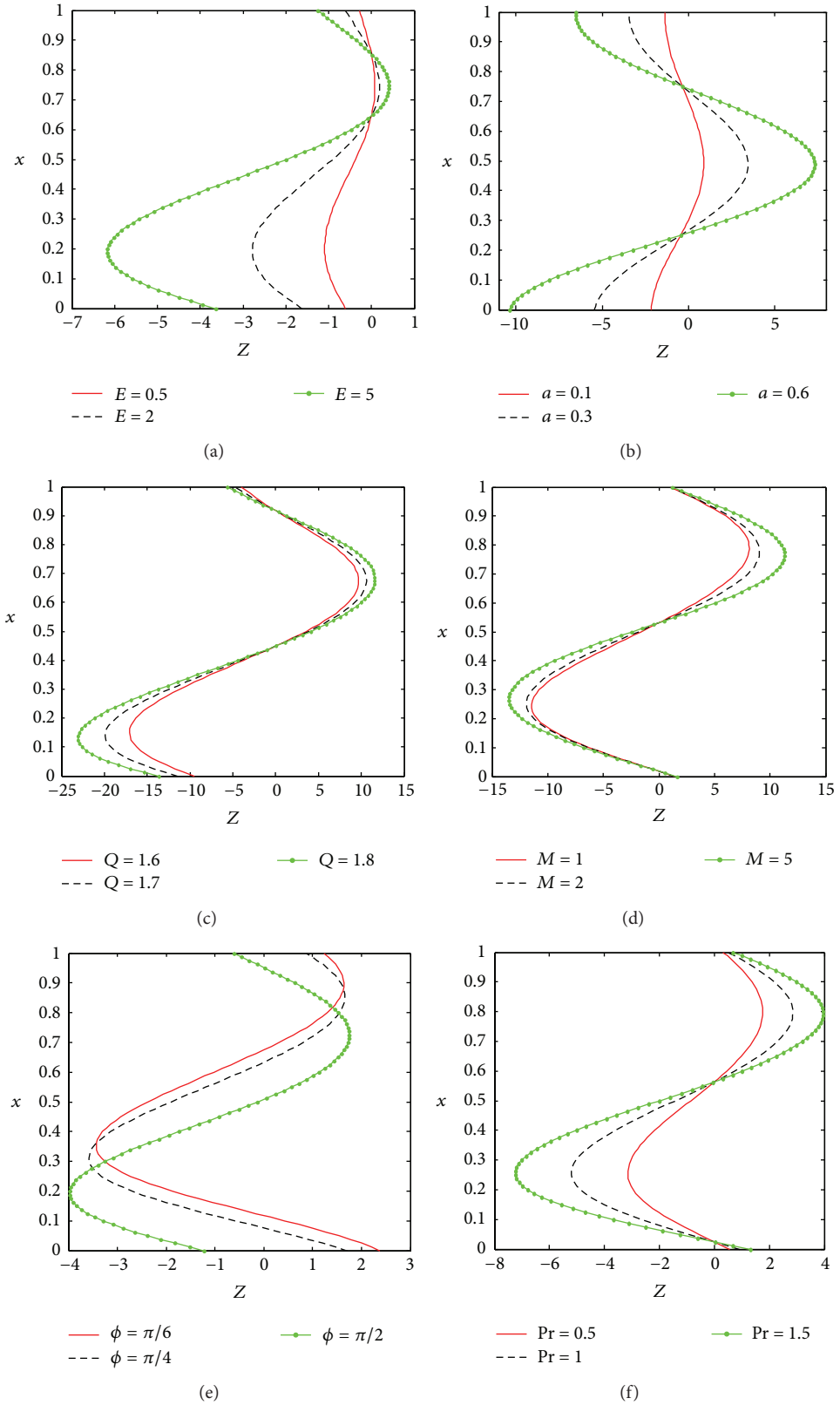

Figure 3: Coefficient of heat transfer distribution: (a) $Q = 1.8$, $\Pr = 0.5$, $k_1 = 0.5$, $M = 3$, $t = 0.5$, $\phi = \pi/2$, $b = 0.2$, and $a = 0.1$; (b) $Q = 1.6$, $M = 0.8$, $t = 0.5$, $\phi = \pi$, $k_1 = 0.2$, $E = 1$, $b = 0.2$, and $\Pr = 1.1$; (c) $t = 0.35$, $E = 2$, $a = 0.4$, $k_1 = 0.25$, $M = 2.5$, $\Pr = 1.5$, $\phi = \pi/3$, $k_1 = 0.1$, and $b = 0.3$; (d) $Q = 1.6$, $t = 0.4$, $\phi = \pi/4$, $E = 2$, $b = 0.35$, $\Pr = 1$, and $a = 0.4$; (e) $Q = 1.78$, $x = 0.48$, $E = 1$, $\Pr = 0.7$, $a = 0.26$, $b = 0.3$, $k_1 = 0.29$, and $M = 1.6$; (f) $Q = 1.72$, $x = 0.42$, $E = 1$, $a = 0.2$, $k_1 = 0.23$, $M = 1.2$, $\phi = \pi/4$, and $b = 0.3$.

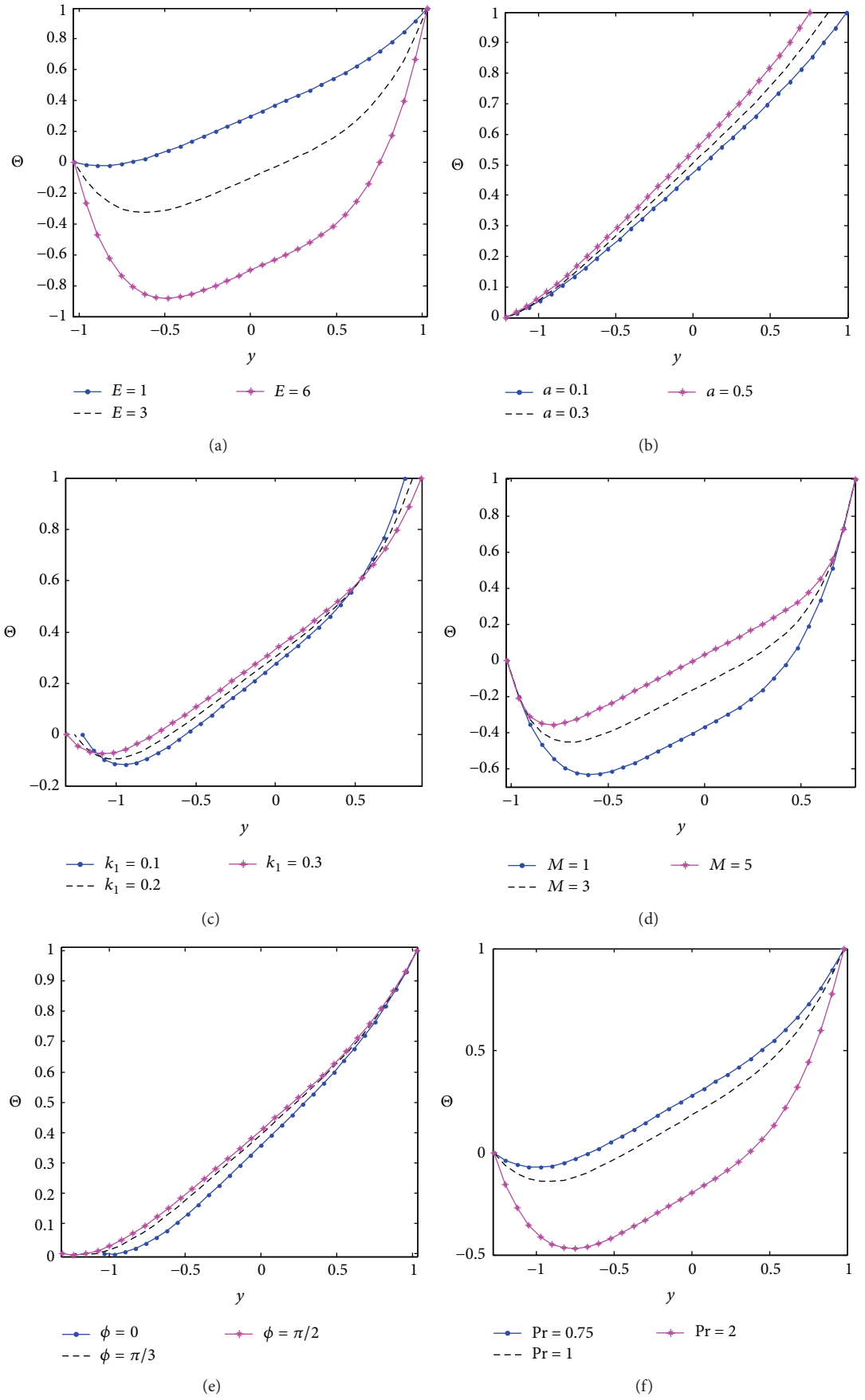

Figure 4: Continued.

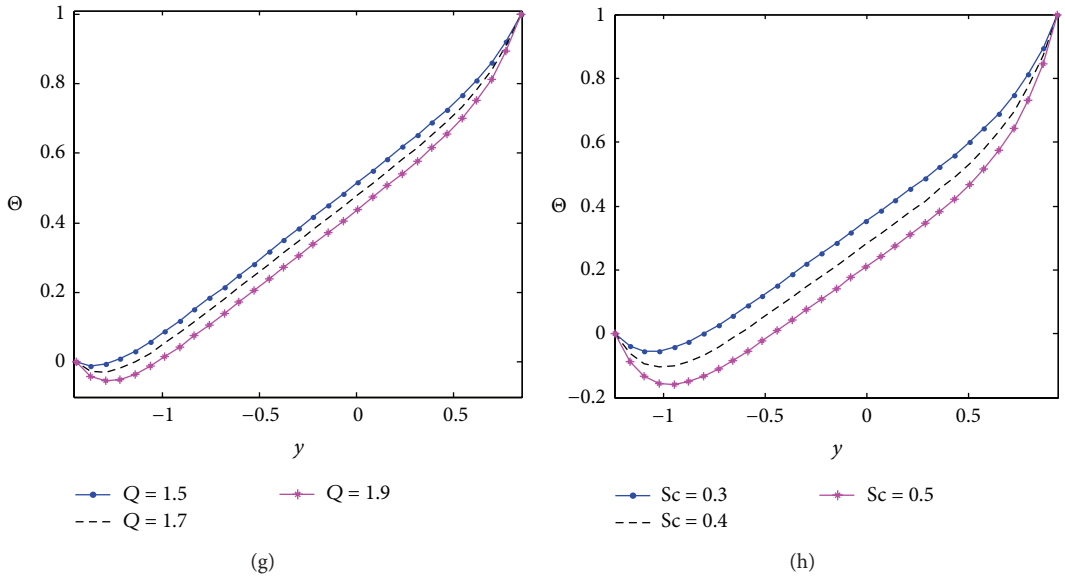

FIGURE 4: Mass transfer distribution (fixed value of $x = 0.5$ and $t = 0.6$): (a) $Q = 1.7$, $a = 0.2$, $b = 0.1$, $\phi = 0$, Pr $= 0.7$, $k_1 = 0.5$, $M = 0.8$, Sc $= 0.6$, and Sr $= 1.6$; (b) $E = 0.5$, $a = 0.2$, $Q = 1.6$, $\phi = \pi/2$, Pr $= 0.5$, $k_1 = 0.1$, $M = 0.5$, Sc $= 0.5$, and Sr $= 1.4$; (c) $a = 0.4$, $b = 0.3$, $E = 1.25$, $Q = 1.65$, $\phi = \pi/3$, Pr $= 1.5$, $M = 0.8$, Sc $= 0.38$, and Sr $= 1.25$; (d) $b = 0.5$, $a = 0.4$, $E = 2$, $Q = 1.55$, $\phi = \pi/6$, Pr $= 2$, $k_1 = 0.15$, Sc $= 0.52$, and Sr $= 1.42$; (e) $b = 0.2$, $a = 0.1$, $E = 0.9$, $Q = 1.8$, Pr $= 0.75$, $k_1 = 0.3$, $M = 0.2$, Sc $= 0.4$, and Sr $= 1.22$; (f) $b = 0.25$, $a = 0.2$, $E = 1.5$, $Q = 1.75$, $\phi = \pi$, $k_1 = 0.25$, $M = 0.5$, Sc $= 0.44$, and Sr $= 1.3$; (g) $a = 0.6$, $b = 0.5$, $E = 0.75$, $\phi = \pi/3$, Pr $= 2$, $k_1 = 0.4$, $M = 3$, Sc $= 0.3$, and Sr $= 1.5$; (h) $b = 0.4$, $a = 0.3$, $E = 1.2$, $Q = 1.65$, $\phi = \pi/4$, Pr $= 1.6$, $M = 2.5$, and Sr $= 1.53$.

detected that with an increase in Pr the concentration of the fluid decreases. Figure 4(g) depicts the concentration profile corresponding to various values of Q. It is seen that the concentration distribution decreases with an increase in the mean flow rate Q. From Figure 4(h), one can view that the concentration profile decreases with increase of Sc.

5. Conclusion

The present analysis can serve as a model which may help in understanding the mechanism of physiological flow of a Newtonian fluid in tapered asymmetric channel. The analytical solutions for the temperature, concentration, and coefficient of heat transfer have been obtained under long wavelength and low Reynolds number approximations. The features of the flow characteristics are analyzed by plotting graphs and discussed in detail. The main observations found from the present study are given as follows.

(1) There is an increase in the temperature (θ) when the Prandtl number Pr, time-average flow rate Q, occlusion parameter a, and Eckert number are increased while it decreases when M is increased.

(2) Mass transfer (Θ) increases with the increase of a, M, and ϕ while it decreases with the increase of E, Pr, Q, and Sc.

(3) The temperature distribution of the fluid increases at the core part of channel when nonuniform parameter is increased and the reverse situation is observed in respect of the concentration of the fluid.

(4) The absolute value of the heat transfer coefficient increases when the E, a, Q, M, ϕ, and Pr are increased.

Conflict of Interests

The authors declare that there is no conflict of interests regarding the publication of this paper.

References

[1] T. W. Latham, *Fluid Motion in a Peristaltic Pump*, MIT Press, Cambridge, Mass, USA, 1966.

[2] A. H. Shapiro, M. Y. Jaffrin, and S. L. Weinberg, "Peristaltic pumping with long wave lengths at low Reynolds number," *Journal of Fluid Mechanics*, vol. 37, no. 4, pp. 799–825, 1969.

[3] G. Radhakrishnamacharya and V. Radhakrishna Murty, "Heat transfer to peristaltic transport in a non-uniform channel," *Defence Science Journal*, vol. 43, no. 3, pp. 275–280, 1993.

[4] T. Hayat, Y. Wang, K. Hutter, S. Asghar, and A. M. Siddiqui, "Peristaltic transport of an Oldroyd-B fluid in a planar channel," *Mathematical Problems in Engineering*, vol. 2004, no. 4, pp. 347–376, 2004.

[5] K. Vajravelu, S. Sreenadh, and V. R. Babu, "Peristaltic transport of a Herschel-Bulkley fluid in an inclined tube," *International Journal of Non-Linear Mechanics*, vol. 40, no. 1, pp. 83–90, 2005.

[6] S. Nadeem, T. Hayat, N. S. Akbar, and M. Y. Malik, "On the influence of heat transfer in peristalsis with variable viscosity," *International Journal of Heat and Mass Transfer*, vol. 52, no. 21-22, pp. 4722–4730, 2009.

[7] T. Hayat, M. U. Qureshi, and Q. Hussain, "Effect of heat transfer on the peristaltic flow of an electrically conducting fluid in

a porous space," *Applied Mathematical Modelling*, vol. 33, no. 4, pp. 1862–1873, 2009.

[8] K. S. Mekheimer, S. Z. A. Husseny, and Y. A. Elmaboud, "Effects of heat transfer and space porosity on peristaltic flow in a vertical asymmetric channel," *Numerical Methods for Partial Differential Equations*, vol. 26, no. 4, pp. 747–770, 2010.

[9] A. Ogulu, "Effect of heat generation on low Reynolds number fluid and mass transport in a single lymphatic blood vessel with uniform magnetic field," *International Communications in Heat and Mass Transfer*, vol. 33, no. 6, pp. 790–799, 2006.

[10] N. T. M. Eldabe, M. F. El-Sayed, A. Y. Ghaly, and H. M. Sayed, "Mixed convective heat and mass transfer in a non-Newtonian fluid at a peristaltic surface with temperature-dependent viscosity," *Archive of Applied Mechanics*, vol. 78, no. 8, pp. 599–624, 2008.

[11] S. Srinivas and M. Kothandapani, "The influence of heat and mass transfer on MHD peristaltic flow through a porous space with compliant walls," *Applied Mathematics and Computation*, vol. 213, no. 1, pp. 197–208, 2009.

[12] S. Srinivas and M. Kothandapani, "Peristaltic transport in an asymmetric channel with heat transfer—a note," *International Communications in Heat and Mass Transfer*, vol. 35, no. 4, pp. 514–522, 2008.

[13] T. A. Ogulu, "Effect of heat generation on low Reynolds number fluid and mass transport in a single lymphatic blood vessel with uniform magnetic field," *International Communications in Heat and Mass Transfer*, vol. 33, no. 6, pp. 790–799, 2006.

[14] O. Eytan, A. J. Jaffa, and D. Elad, "Peristaltic flow in a tapered channel: application to embryo transport within the uterine cavity," *Medical Engineering and Physics*, vol. 23, no. 7, pp. 473–482, 2001.

[15] M. Kothandapani and J. Prakash, "The peristaltic transport of Carreau nanofluids under effect of a magnetic field in a tapered asymmetric channel: application of the cancer therapy," *Journal of Mechanics in Medicine and Biology*, vol. 15, Article ID 1550030, 2014.

[16] M. Kothandapani and J. Prakash, "Effect of radiation and magnetic field on peristaltic transport of nanofluids through a porous space in a tapered asymmetric channel," *Journal of Magnetism and Magnetic Materials*, vol. 378, pp. 152–163, 2015.

[17] L. M. Srivastava, V. P. Srivastava, and S. N. Sinha, "Peristaltic transport of a physiological fluid. Part-I. Flow in non-uniform geometry," *Biorheology*, vol. 20, no. 2, pp. 153–166, 1983.

[18] M. Kothandapani and J. Prakash, "Influence of heat source, thermal radiation and inclined magnetic field on peristaltic flow of a Hyperbolic tangent nanofluid in a tapered asymmetric channel," *IEEE Transactions on NanoBioscience*, 2014.

[19] M. Kothandapani and J. Prakash, "Effects of thermal radiation parameter and magnetic field on the peristaltic motion of Williamson nanofluids in a tapered asymmetric channel," *International Journal of Heat and Mass Transfer*, vol. 81, pp. 234–245, 2015.